Motion Planning for Two 3D–Dubins Vehicles with Distance Constraint

Hamal Marino*†, Marco Bonizzato*o†, Riccardo Bartalucci*†, Paolo Salaris‡, Lucia Pallottino‡

Abstract— **In this paper we consider the motion planning problem for a *3D–Dubins* system consisting of a pair of Dubins vehicles moving in a 3D space while maintaining constant distance. We provide a motion planning algorithm and sufficient conditions on the initial and final configurations that guarantee the existence of admissible controls, moving a first step towards the complete controllability characterization of such type of systems. Results obtained in this paper are particularly relevant in order to solve formation control problem for multiple robots as aerial or underwater vehicles, which move in 3D spaces. Simulation results demonstrate the feasibility of the motion planning algorithm proposed in this paper.**

I. Introduction

The formation control problem for multiple robots has been extensively studied in the literature (see [1] for a detailed review and references therein). Formation control studies the problem of controlling multiple robots so that they can maintain some given configuration constraints (e.g. distances) while moving as a whole group [2], [3], [4]. Moving in formation has many advantages, for example, it can reduce the energy consumption and can increase the robustness and efficiency, providing at the same time redundancy and flexibility for the system [5], [1]. Also in nature, several types of animals, such as insects, birds, or fishes, aggregate together, moving *en masse* or migrating in some directions, known as swarm behavior. The term shoaling or schooling is used to refer specifically to swarm behavior in fishes which derive many benefits including also the increased hydrodynamic efficiency (cf. [6]).

Many approaches of formation control have been proposed, such as behavior-based methods [7], leader-follower strategies [8], [9] and virtual structure approaches [10]. Various kinds of nonholonomic vehicles have been considered, such as ground vehicles (e.g. in [11]), aircraft (e.g. in [12]) and underwater vehicles (e.g. in [13]).

However, in order to solve challenging problems, e.g. motion planning algorithms, control law design, formation stability properties, and optimal trajectories, especially for complex systems such as multiple robots moving as a whole, it is important to analyze the controllability properties first. A system is completely controllable if, for every pair of points q_1 and q_2 in the configuration space, there exists a control that steers the system from q_1 to q_2 (see [14], [15]). This is an important condition for the design of motion planning algorithms and for the existence of an optimal trajectory. In [16] the controllability of different pairs of identical nonholonomic vehicles moving in a plane while maintain a constant distance has been proved. Results obtained have then been used in order to prove controllability and design a motion planning algorithm for formation of planar Dubins vehicles [12], [17]. In this paper our purpose is to extend results of [17] to a *3D–Dubins* system consisting of a pair of Dubins vehicles moving in a 3D space while maintaining constant distance. As in the aforementioned works, also for the system considered in this paper, the challenge is that the control input set depends on the system configurations and classical controllability results can not be directly applied. Hence, first a definition of feasible configurations is provided to characterize configurations from which an admissible control exists. The main contribution of this paper is the proof that the feasibility of the initial and final configurations is sufficient to guarantee the existence of admissible controls. This result is fundamental to move a first step towards the complete controllability characterization of such type of systems. Furthermore, a motion planning algorithm to drive such a system from any initial to any final feasible configuration is presented.

The characterization of necessary conditions for controllability is still an open problem. Anyway, the present work can be exploited to solve several open problems such as motion planning and optimal planning for more complex formations of robots in 3D space, as many biological beings do in nature.

II. Modeling

Consider a nonholonomic vehicle moving in a three dimensional space and let $\langle W \rangle = (O_w,\, X_w,\, Y_w,\, Z_w)$ be a fixed frame. In $\langle W \rangle$, the vehicle configuration is $\zeta(t) = (x(t),\, y(t),\, z(t),\, \varphi(t),\, \psi(t))$ where $\boldsymbol{q} = (x(t),\, y(t),\, z(t))$ is the position in $\langle W \rangle$ of the reference central point in the vehicle, $\varphi(t)$ is the angle formed by the vehicle heading and the plane $X_w \times Y_w$ and $\psi(t)$ is the angle formed by the projection of the vehicle heading on the plane $X_w \times Y_w$ and X_w axis (see figure 1).

Given the forward velocity v of the vehicle, the velocity vector $\boldsymbol{v}$ in $\langle W \rangle$ is $\boldsymbol{v} = (v\cos\varphi\sin\psi,\, v\cos\varphi\cos\psi,\, v\sin\varphi)^T$. The kinematic model of the nonholonomic vehicle is (cf. [18])

$$\begin{cases} \dot{\boldsymbol{q}} = \boldsymbol{v} \\ \dot{\boldsymbol{v}} = \boldsymbol{v} \times \boldsymbol{\omega} \end{cases} \tag{1}$$

where $\boldsymbol{\omega} = (\dot{\psi},\, \dot{\varphi}\sin\psi,\, -\dot{\varphi}\cos\psi)^T$.

This work was supported by E.C. contracts n.224053 CONET (Cooperating Objects Network of Excellence), n. 257462 HYCON2 (Network of Excellence) and n.2577649 PLANET.

* are with Scuola Superiore Sant'Anna - Piazza Martiri della Libertà, 33 - 56127 Pisa.

o is also with l'École polytechnique fédérale de Lausanne (EPFL), Switzerland.

‡ are with the Interdept. Research Center,"Enrico Piaggio", University of Pisa, via Diotisalvi 2, 56100 Pisa, Italy.

† These authors equally contributed to this work and should be considered co-first authors.

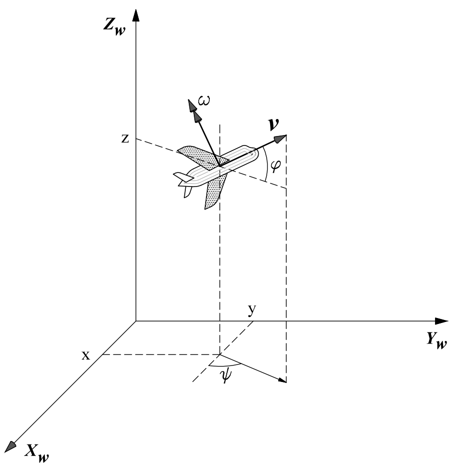

Fig. 1. Representation of a vehicle in a 3D space

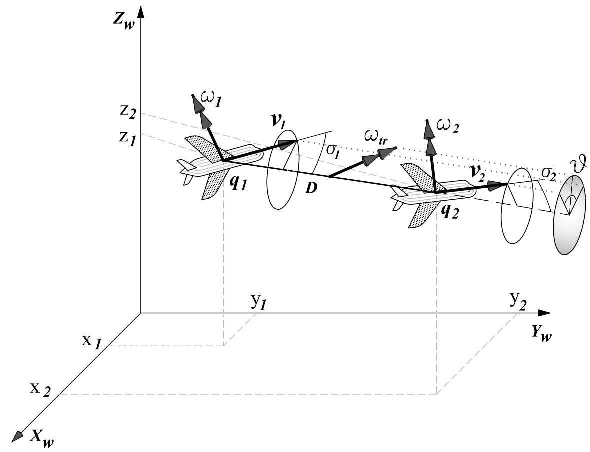

Fig. 2. Configuration of the *3D–Dubins* system

In the rest of the paper, we denote with $\hat{\omega}$ the skew-symmetric matrix associated to the cross product

$$\hat{\omega} = \begin{bmatrix} 0 & \omega_z & -\omega_y \\ -\omega_z & 0 & \omega_x \\ \omega_y & -\omega_x & 0 \end{bmatrix}, \tag{2}$$

where $\boldsymbol{\omega} = (\omega_x, \omega_y, \omega_z)$, i.e. $\boldsymbol{v} \times \boldsymbol{\omega} = \hat{\omega}\boldsymbol{v}$. Notice that, since the control $\boldsymbol{\omega}$ can only rotate $\boldsymbol{v}$, the velocity $\boldsymbol{v}$ has constant modulus v.

In this paper we consider the *3D–Dubins* system that is described by (1) and a constrained control effort

$$|\boldsymbol{\omega}| \leq \omega_M. \tag{3}$$

Moreover, without loss of generality, we consider $v = 1$. In such conditions, a *3D–Dubins* generates trajectories with bounded curvature, as the minimum radius is $R = \frac{v}{\omega_M}$.

A. Problem definition

Consider the system consisting of a pair of *3D–Dubins* constrained to maintain constant the magnitude D of the distance vector $\boldsymbol{D}$ joining the centers of the two robots. Referring to figure 2, let $\boldsymbol{q}_i$, $\boldsymbol{v}_i$ and $\boldsymbol{\omega}_i$ be the position, forward and angular velocity vectors of vehicle i, $i = 1, 2$, respectively. Furthermore, let $\sigma_i \in [0, \pi]$ be the angle between $\boldsymbol{v}_i$ and $\boldsymbol{D}$ ($i = 1, 2$) and let $\theta \in [0, \pi]$ be the angle between the projections of $\boldsymbol{v}_1$ and $\boldsymbol{v}_2$ on the plane orthogonal to $\boldsymbol{D}$. Notice that, when $\boldsymbol{v}_i$ are aligned with $\boldsymbol{D}$, θ is not defined while is zero if $\boldsymbol{v}_i$ are parallel. In the following we will refer to $\theta = 0$ also when σ_1 or σ_2 are zero with an abuse of notation.

The constraint is to keep constant the magnitude of vector $\boldsymbol{D} = \boldsymbol{q}_2 - \boldsymbol{q}_1$, i.e. $\dot{\boldsymbol{D}} = \boldsymbol{v}_2 - \boldsymbol{v}_1$ must be always orthogonal to $\boldsymbol{D}$. Equivalent equations of the distance constraint are

$$\dot{\boldsymbol{D}} \cdot \boldsymbol{D} = 0, \tag{4a}$$

$$\boldsymbol{D} \cdot (\boldsymbol{v}_2 - \boldsymbol{v}_1) = 0, \tag{4b}$$

Given initial and final configurations, the goal of this paper is then to provide a motion planning algorithm for the system of a pair of 3D–Dubins subject to (4):

$$\begin{cases} \dot{\boldsymbol{q}}_1 = \boldsymbol{v}_1 \\ \dot{\boldsymbol{q}}_2 = \boldsymbol{v}_2 \\ \dot{\boldsymbol{v}}_1 = \boldsymbol{v}_1 \times \boldsymbol{\omega}_1 \\ \dot{\boldsymbol{v}}_2 = \boldsymbol{v}_2 \times \boldsymbol{\omega}_2 \end{cases}, \tag{5}$$

B. Angular velocity of $\boldsymbol{D}$

Let $\boldsymbol{\omega}_{\text{tr}}$ be the angular velocity of $\boldsymbol{D}$, i.e. $\dot{\boldsymbol{D}} = \boldsymbol{D} \times \boldsymbol{\omega}_{\text{tr}}$ or equivalently

$$\boldsymbol{D} \times \boldsymbol{\omega}_{\text{tr}} = \boldsymbol{v}_2 - \boldsymbol{v}_1. \tag{6}$$

Remark 1: It is worth noting that $\boldsymbol{\omega}_{\text{tr}}$ does not change the magnitude D of $\boldsymbol{D}$. The component of $\boldsymbol{\omega}_{\text{tr}}$ along $\boldsymbol{D}$, representing the rotation of $\boldsymbol{D}$ with respect to its own axis, does not affect the system configuration. Hence, in the rest of the paper we will assume an angular velocity $\boldsymbol{\omega}_{\text{tr}}$ such that

$$\boldsymbol{\omega}_{\text{tr}} \cdot \boldsymbol{D} = 0. \tag{7}$$

Remark 2: From (6) we have

$$\boldsymbol{\omega}_{\text{tr}} \cdot (\boldsymbol{v}_2 - \boldsymbol{v}_1) = 0, \tag{8}$$

hence the angular velocity of $\boldsymbol{D}$ is always orthogonal to $\boldsymbol{v}_2 - \boldsymbol{v}_1$. Furthermore, the projection of $\boldsymbol{\omega}_{\text{tr}}$ and of $\boldsymbol{v}_i$ along the plane orthogonal to $\boldsymbol{D}$ form an angle $\theta/2$.

Moreover, when $\sigma_1 = \sigma_2 = \sigma$ (as will occur in the following to maintain the given distance), from (6) and Remark 1

$$\omega_{\text{tr}} = \frac{|\boldsymbol{v}_2 - \boldsymbol{v}_1|}{D} = \frac{2 \sin\frac{\theta}{2} \sin\sigma}{D}. \tag{9}$$

C. Control constraints

We now show the effect of the distance constraints (4) in terms of constraints on the controls.

It will be useful, in the rest of the paper, to consider the control $\boldsymbol{\omega}_i$ written as

$$\boldsymbol{\omega}_i = \boldsymbol{\omega}_{\text{tr}} + \boldsymbol{\omega}_{r,i}, \tag{10}$$

where $\boldsymbol{\omega}_{r,i}$ is the relative control that it is not necessarily orthogonal to $\boldsymbol{\omega}_{\text{tr}}$. Notice that $\boldsymbol{\omega}_{\text{tr}}$ represents the component of the control that is common to both vehicles due to the distance constraints. In the following we will refer to $\boldsymbol{\omega}_{\text{tr}}$ also as the *dragging control* component. The choice of $\boldsymbol{\omega}_{r,i}$ is then constrained only by the admissibility condition. Indeed, the value ω_{tr} depends on the system configuration as described in (9) and $\omega_{r,i}$ must be chosen in order to guarantee that ω_i verify the control constraint (3).

Remark 3: Starting from configurations in which $|\boldsymbol{\omega}_{tr}| \leq \omega_M$ and applying admmissible controls $\boldsymbol{\omega}_1 = \boldsymbol{\omega}_2 = \boldsymbol{\omega}_{\text{tr}}$ (i.e. considering $\boldsymbol{\omega}_{r,1} = \boldsymbol{\omega}_{r,2} = 0$) σ_1, σ_2 and θ are constant during system evolution. Indeed, the same rotational velocity is applied to $\boldsymbol{v}_1$, $\boldsymbol{v}_2$, and to $\boldsymbol{D}$, making the system rotating as a whole, and keeping the internal configuration constant.

The distance constraint limits admissible configurations and controls that can be imposed to vehicles.

Proposition 1: Necessary conditions on system configurations and controls to guarantee the distance constraint (4) are

$$\sigma_1 = \sigma_2 \triangleq \sigma, \tag{11}$$

$$\boldsymbol{D} \cdot (\boldsymbol{v}_1 \times \boldsymbol{\omega}_{r,1}) = \boldsymbol{D} \cdot (\boldsymbol{v}_2 \times \boldsymbol{\omega}_{r,2}). \tag{12}$$

Proof: From (4b) we have that $\boldsymbol{v}_1$ and $\boldsymbol{v}_2$ must have equal components along $\boldsymbol{D}$, i.e. $v_1 \cos\sigma_1 = v_2 \cos\sigma_2$.

Taking the time derivative of (4b) and using (10) we have

$$\begin{aligned} \hat{\omega}_{\text{tr}}\boldsymbol{D} \cdot (\boldsymbol{v}_2 - \boldsymbol{v}_1) + \boldsymbol{D} \cdot \hat{\omega}_{\text{tr}}(\boldsymbol{v}_2 - \boldsymbol{v}_1) + & \\ \boldsymbol{D} \cdot (\hat{\omega}_{r,2}\boldsymbol{v}_2 - \hat{\omega}_{r,1}\boldsymbol{v}_1) &= 0. \end{aligned} \tag{13}$$

Since $\hat{\omega}_{\text{tr}}$ is skew-symmetric the first two addenda of (13) cancel out and we get $\boldsymbol{D} \cdot \hat{\omega}_{r,2}\boldsymbol{v}_2 = \boldsymbol{D} \cdot \hat{\omega}_{r,1}\boldsymbol{v}_1$, hence the thesis. ■

Definition 1: A configuration $\boldsymbol{\xi} = (\boldsymbol{q}_1, \boldsymbol{q}_2, \boldsymbol{v}_1, \boldsymbol{v}_2)$ of *3D–Dubins* will be called *feasible* if $\sigma_1 = \sigma_2$ and $\omega_{\text{tr}} = \frac{2\sin\frac{\theta}{2}\sin\sigma}{D} < \omega_M$.
Such configurations will be the main focus of the rest of the paper: it will be proved that there always exists an admissible control steering the system between any two of them (section V). Next sections (III and IV) will thus provide basic maneuvers to steer the system between generic feasible configurations.

III. Basic Movements

In order to get a complete motion planning algorithm for a *3D–Dubins* pair, it is convenient to start investigating some basic movements and eventually connect them to form the complete path. The ideas behind the choice of basic movements and the associated controls, described next, are:
1) to steer the system with planar movements when possible (i.e. velocities and distance vectors lie on one plane),
2) to obtain basic controls that allow to reach the desired configuration without violating the control's admissibility condition given by (3).
Furthermore, a feasible initial configuration is considered so that distance constraint is initially verified.

A. Steering of θ and σ to zero

In the motion planning it is necessary to rotate and translate $\boldsymbol{D}$ from initial to final configuration. In terms of control admissibility, it is a good choice to translate and rotate $\boldsymbol{D}$ from a configuration with both $\sigma = 0$ and $\theta = 0$. Furthermore, with this choice, desired translation and rotation of $\boldsymbol{D}$ can be obtained separately with planar movements.

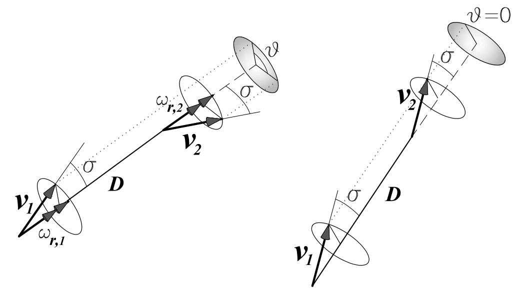

Fig. 3. Steering θ to zero (keeping constant σ)

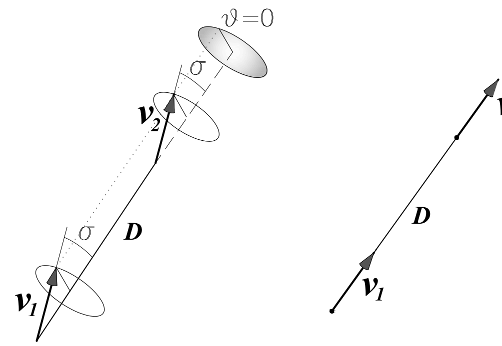

Fig. 4. Steering σ to zero (keeping constant $\theta = 0$)

To steer θ to zero, consider $\boldsymbol{\omega}_{r,1}$ and $\boldsymbol{\omega}_{r,2}$ aligned along $\boldsymbol{D}$ so that the effect of relative controls on $\boldsymbol{D}$ is a rotation around its own axis and the distance constraint is not violated. $\boldsymbol{\omega}_{r,1}$ and $\boldsymbol{\omega}_{r,2}$ are then chosen with opposite direction in order to decrease θ to zero, (see figure 3). Notice that, from (9), with this choice of $\boldsymbol{\omega}_{r,i}$, ω_{tr} decreases when θ does. It is hence sufficient to choose $\omega_{r,i}$ so that the control constraint (3) is verified considering the value of ω_{tr} in the initial configuration.

Once $\theta = 0$, in order to align the two *3D–Dubins* on the distance vector (see figure 4), thus to rotate the vectors $\boldsymbol{v}_i$ towards $\boldsymbol{D}$ or equivalently to steer σ to zero, it is sufficient to choose relative controls $\boldsymbol{\omega}_{r,i}$ orthogonal to $\boldsymbol{v}_i$ and $\boldsymbol{D}$, $i = 1, 2$. In order to verify the distance constraint it is necessary to choose relative controls with equal magnitude so that $\sigma_1 = \sigma_2 = \sigma$ during evolution. It is important to notice that, $\theta \equiv 0$ (i.e. $\boldsymbol{\omega}_{tr} = 0$) and hence $\omega_{r,i} = \omega_M$ lead to an admissible control.

Notice that, steering σ to zero, from a configuration with $\theta \neq 0$, may increase the value of ω_{tr} limiting the choice of $\omega_{r,i}$ to verify the control constraint (3). For example, referring to (9), from a configuration with $\sigma > \pi/2$, while controls $\omega_{r,i}$ are chosen to decrease σ to zero, the value of ω_i increases with ω_{tr} toward the admissible upper bound. The proposed strategy to first steer θ to zero is hence a conservative maneuver able to guarantee control constraints.

B. Translation of $\boldsymbol{D}$ on a plane

When $\theta = 0$, (9) implies $\boldsymbol{\omega}_{tr} = 0$. Hence, controls

$\boldsymbol{\omega}_1 = \boldsymbol{\omega}_2$ (with $\omega_i \leq \omega_M$, $i = 1, 2$) steer the system on the plane containing $\boldsymbol{D}$, $\boldsymbol{v}_1$ and $\boldsymbol{v}_2$, and orthogonal to $\boldsymbol{\omega}_1$ and $\boldsymbol{\omega}_2$. Notice that, during the evolution, $\theta \equiv 0$ and hence $\boldsymbol{D}$ is translated on the plane. Notice that $\boldsymbol{\omega}_1 = \boldsymbol{\omega}_2$ implies $\sigma_1 = \sigma_2$ during system evolution, thus verifying the distance constraint.

C. Rotation of $\boldsymbol{D}$ on a plane

In order to make $\boldsymbol{D}$ rotating in the space it is necessary to have $\boldsymbol{\omega}_{tr} \neq 0$. Hence, when $\theta = 0$, controls $\boldsymbol{\omega}_1$ and $\boldsymbol{\omega}_2$ parallel and with $\omega_1 = -\omega_2$ must be applied to obtain a rotation of $\boldsymbol{D}$. Notice that applying such maneuver $\theta = \pi$ as long as $\sigma \neq 0$. Choosing, $\boldsymbol{\omega}_i$ orthogonal to $\boldsymbol{v}_i$ and $\boldsymbol{D}$, the system will evolve along the plane containing $\boldsymbol{D}$ and $\boldsymbol{v}_i$. Furthermore, $\omega_1 = -\omega_2$ implies that $\sigma_1 = \sigma_2 = \sigma$ verifying the distance constraint.

To rotate $\boldsymbol{D}$ of a given quantity ν, we are interested in determining the controls of both vehicles (additional to $\boldsymbol{\omega}_{tr}$) with magnitude $|\omega_{r,1}| = |\omega_{r,2}|$ such that, at the end, the desired rotation is obtained. Indeed, the value of ω_{tr} depends on θ and σ and, when not null, it rotates $\boldsymbol{D}$. Hence, $\omega_{r,1}$ and $\omega_{r,2}$ are first used to let $\theta = \pi$ and then give a non null angular velocity to $\boldsymbol{D}$. Finally, opposite values of $\omega_{r,1}$ and $\omega_{r,2}$ can be used to drive back σ (and hence θ) to zero and stop the rotation of $\boldsymbol{D}$. During the phase in which θ and σ are incremented, the consequently increasing magnitude of $\boldsymbol{\omega}_{tr}$, added to the control variables $\boldsymbol{\omega}_{r,i}$, may saturate the constraint (3). In this case it is possible to let the system evolve with only $\boldsymbol{\omega}_{tr}$ while $\omega_{r,i} = 0$. More formally, a possible choice of the controls is

1) $\omega_{r,1} = -\omega_{r,2} = \varepsilon$ for $t \in [0, \delta)$;
2) $\omega_{r,1} = \omega_{r,2} = 0$ for $t \in [\delta, \bar{t} - \delta)$;
3) $\omega_{r,1} = -\omega_{r,2} = -\varepsilon$ for $t \in [\bar{t} - \delta, \bar{t}]$,

the value ε is chosen to be as small as needed in order to let ω_{tr} have a non zero magnitude while still respecting the constraint (3). δ is chosen to be the minimum between the time needed to obtain a rotation of $\frac{\nu}{2}$, and the time needed to reach a dragging control value of $\omega_{tr} = \omega_M - \varepsilon$ to guarantee admissibility of the control variable $\boldsymbol{\omega}_i$.

If a rotation of $\frac{\nu}{2}$ is obtained before the control saturation occurs, $\bar{t}$ is chosen to be 2δ and the second step is not performed (i.e. the *null* control is never used). Otherwise, let $\bar{\nu}$ be the rotation realized in step 1, the time $\bar{t}$ of step 2, during which the system rotate with fixed θ and σ, is such that the total rotation performed in step 2 and step 3 is $\nu - \bar{\nu}$.

The admissibility of the controls chosen in this movement will be further discussed in section V, theorem 1.

IV. Motion planning

A. Reverse System

To complete the motion planning, we define the *reverse system* of *3D–Dubins* introduced in Section II as follows:

$$\begin{cases} \dot{\boldsymbol{q}}_1^R = -\boldsymbol{v}_1^R \\ \dot{\boldsymbol{q}}_2^R = -\boldsymbol{v}_2^R \\ \dot{\boldsymbol{v}}_1^R = -\boldsymbol{v}_1^R \times \boldsymbol{\omega}_1^R \\ \dot{\boldsymbol{v}}_2^R = -\boldsymbol{v}_2^R \times \boldsymbol{\omega}_2^R. \end{cases} \tag{14}$$

All symbols and subscripts are consistent to what we defined in (5). The only difference stands in the changed signs in the dynamics evolution.

In addition, the constraints represented by (3)-(4) also apply to this model with the appropriate variable substitution (e.g., $\boldsymbol{q}_1^R$ in place of $\boldsymbol{q}_1$).

Remark 4: Applying to the *3D–Dubins* system the control $\boldsymbol{\omega}(t)$, from $\boldsymbol{\xi}(t_0) = (\boldsymbol{q}_1(t_0), \boldsymbol{q}_2(t_0), \boldsymbol{v}_1(t_0), \boldsymbol{v}_2(t_0))$ a configuration $\boldsymbol{\xi}(t_f) = (\boldsymbol{q}_1(t_f), \boldsymbol{q}_2(t_f), \boldsymbol{v}_1(t_f), \boldsymbol{v}_2(t_f))$ is reached in $t = t_f$. In the reverse system, starting from $\boldsymbol{\xi}^R(t_0) = \boldsymbol{\xi}(t_f)$ and applying control $\boldsymbol{\omega}^R(t) = \boldsymbol{\omega}(t_f - t)$ (i.e. the *reverse* control law) the position $\boldsymbol{\xi}^R(t_f) = \boldsymbol{\xi}(t_0)$ is obtained.

We will use this property in the next section to ease the design of a motion planning algorithm based only on the basic movements described in section III.

B. Motion Planning Algorithm

In this section we develop a possible algorithm for the motion planning of a 3D–Dubins couple with arbitrary start and final configurations respecting the constraint (11). The feasibility of this algorithm will then be further addressed in Section V.

Indicating with $\boldsymbol{u} = (\boldsymbol{\omega}_1, \boldsymbol{\omega}_2)$ and as $\boldsymbol{u}^R = (\boldsymbol{\omega}_1^R, \boldsymbol{\omega}_2^R)$ the controls of the original and reverse systems, respectively, and given two feasible configurations $\boldsymbol{\xi}_s = \boldsymbol{\xi}(t_0)$ and $\boldsymbol{\xi}_f = \boldsymbol{\xi}(t_f)$, the algorithm is structured as follows:

1) steer the system towards a configuration ${}^a\boldsymbol{\xi}_s$ in which vehicles are aligned to the distance vector (i.e. $\sigma = 0$; hereafter we use the superscript a to denote that vehicles are aligned with $\boldsymbol{D}$), applying a control $\boldsymbol{u}_1$ as described in section III-A;
2) apply step 1 to the reverse system, from $\boldsymbol{\xi}_f$ to a configuration ${}^a\boldsymbol{\xi}_f$ using a control $\boldsymbol{u}_2^R$; *reverse* it to obtain $\boldsymbol{u}_2$;
3) from ${}^a\boldsymbol{\xi}_s$ steer the system towards ${}^a\boldsymbol{\xi}$, a configuration in which the distance vector is parallel to the one of ${}^a\boldsymbol{\xi}_f$, applying a control $\boldsymbol{u}_3$ as described in section III-C;
4) steer the system from ${}^a\boldsymbol{\xi}$ to ${}^a\boldsymbol{\xi}_f$ through a *parallel Dubins path* applying a control $\boldsymbol{u}_4$ as described in section III-B and similar to the one described in [17]. Such control steers both vehicles with the same control $\boldsymbol{\omega}_i$ translating the distance vector in space along two parallel trajectories consisting in concatenations of straight lines and curves of limited curvature to verify the control constraint (3).
5) use the control $\boldsymbol{u}_2$ to steer the system from ${}^a\boldsymbol{\xi}_f$ to $\boldsymbol{\xi}_f$.

Refer to figure5 for a visual representation of the motion planning steps.

In summary, the steps are:

$$\boldsymbol{\xi}_s \xrightarrow{\boldsymbol{u}_1} {}^a\boldsymbol{\xi}_s \xrightarrow{\boldsymbol{u}_3} {}^a\boldsymbol{\xi} \xrightarrow{\boldsymbol{u}_4} {}^a\boldsymbol{\xi}_f \xrightarrow{\boldsymbol{u}_2} \boldsymbol{\xi}_f$$

In figure 7 the path from $\boldsymbol{q}_s = (\boldsymbol{q}_1(t_0)^T, \boldsymbol{q}_2(t_0)^T)^T = (0, 0, 0, 3, 0, 0)^T$ to $\boldsymbol{q}_f = (\boldsymbol{q}_1(t_f)^T, \boldsymbol{q}_2(t_f)^T)^T = (0, 0, 4, 0, 3, 4)^T$ with $\boldsymbol{v}_1(t_0) = (0, 0, 1)^T$, $\boldsymbol{v}_2(t_0) = (0, 0, -1)^T$, $\boldsymbol{v}_1(t_f) = (-1, 0, 0)^T$ and $\boldsymbol{v}_2(t_f) = (1, 0, 0)^T$ is represented. Furthermore, a maximum control magnitude of 1 has been considered.

Finally, in figure 6 the steps of the algorithm for the path of figure 7 are represented.

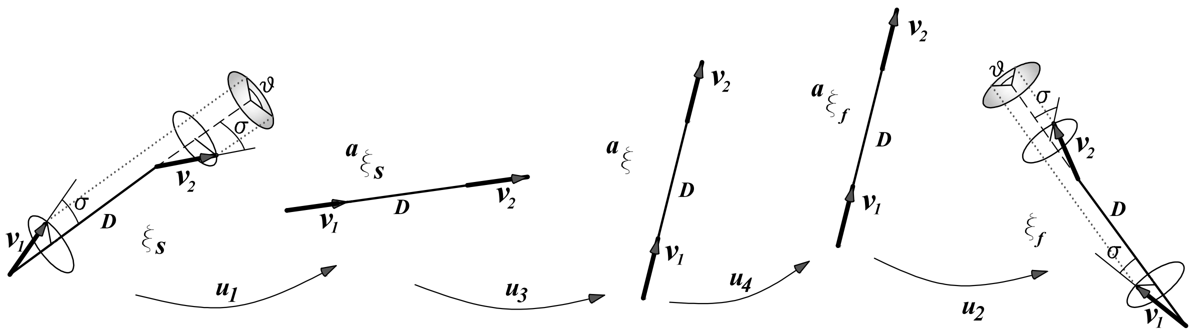

Fig. 5. Motion Planning Steps

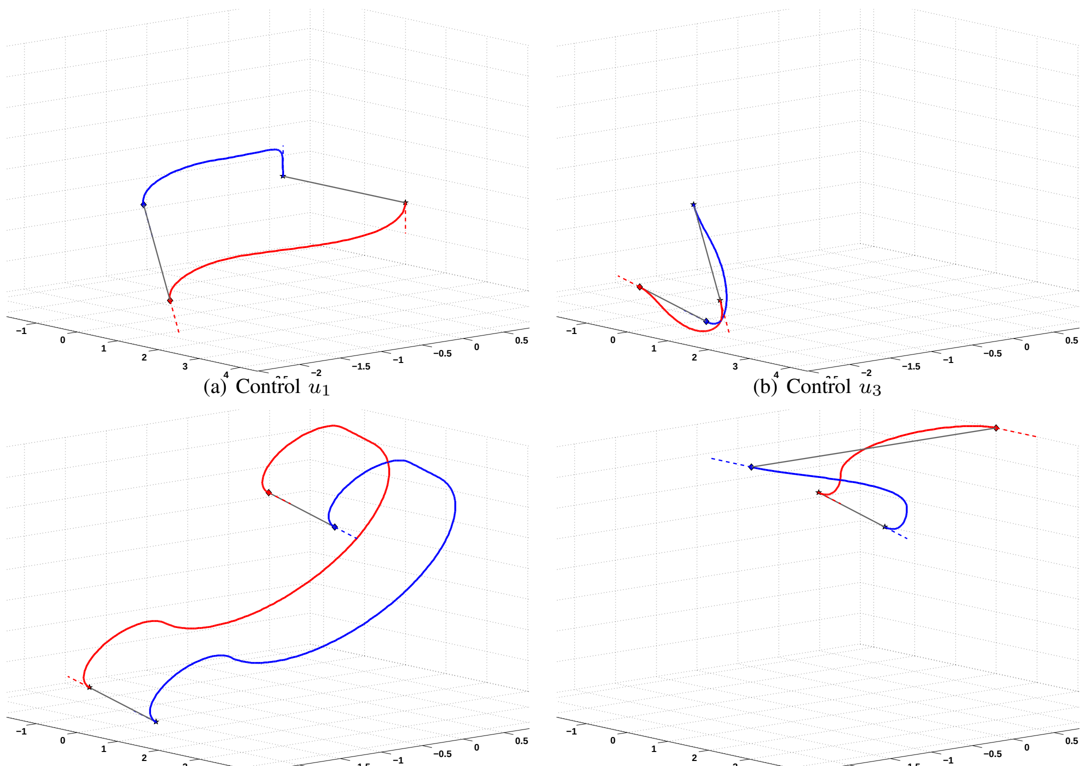

(a) Control u_1

(b) Control u_3

(c) Control u_4

(d) Control u_2

Fig. 6. Steps of path represented in figure 7

V. Sufficient Conditions for Controllability

Theorem 1: Given *feasible* initial and final configurations $\boldsymbol{\xi}_s$ and $\boldsymbol{\xi}_f$ of *3D–Dubins*, there always exist a control law $\boldsymbol{u} = (\boldsymbol{\omega}_1, \boldsymbol{\omega}_2)$ such that $\omega_i \leq \omega_M$, $i = 1, 2$ that steers the system from $\boldsymbol{\xi_s}$ to $\boldsymbol{\xi}_f$.

Proof: To prove the existence of control laws that verify the constraint (3), we chose the controls determined in the proposed motion planning algorithm. It is worth noticing that any configuration reached from a feasible one with admissible control is a feasible configuration.

As shown in section III-A, the control $\boldsymbol{u}_1$ (Step 1 of Motion Planning algorithm), that steers the system from $\boldsymbol{\xi}_s$ to a configuration ${}^a\boldsymbol{\xi}_s$ with $\theta = \sigma = 0$ consists of two parts. The first part, dedicated to position $\boldsymbol{v}_1$ and $\boldsymbol{v}_2$ on parallel lines, is performed with controls $\omega_{r,i} \neq 0$ such that for the initial configuration $\omega_i \leq \omega_M$, $i = 1$ and 2. Such controls exist in the feasible initial configuration since $\omega_{tr} < \omega_M$. Furthermore, during evolution, ω_{tr} decreases with θ and hence (3) is always verified.

The second part, dedicated to align $\boldsymbol{v}_i$ along $\boldsymbol{D}$, is performed with controls $\omega_{r,i} \neq 0$ while $\omega_{tr} = 0$. Hence, it is sufficient to choose $\omega_{r,i} \leq \omega_M$ to verify (3).

With the same reasoning, the control $\boldsymbol{u}_2$ (Steps 2 and 4 of Motion Planning algorithm) verify (3) since $\boldsymbol{\xi}_f$ is feasible.

In Step 3, the maneuver described in III-C is considered choosing, initially, controls $\omega_{r,1} = -\omega_{r,2} = \varepsilon < \omega_M$ from the feasible configuration reached after Step 1.

Notice that during evolution $\theta = \pi$ while the value of $\omega_{tr} = \frac{2 \sin \sigma}{D}$ increases with σ. If the controls $\omega_i < \omega_M - \varepsilon$, the system is then steered to the desired orientation of $\boldsymbol{D}$

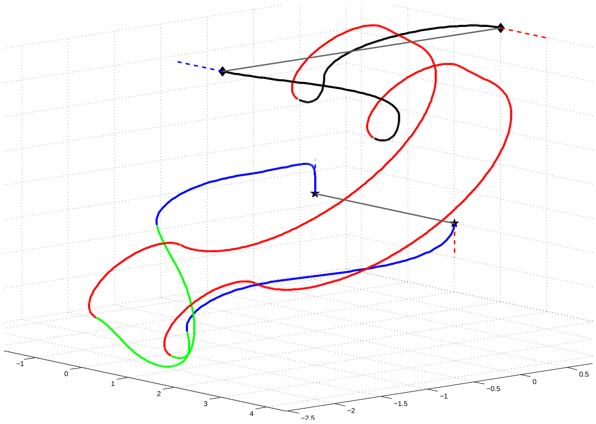

Fig. 7. Path obtained from $\boldsymbol{q}_s = (0, 0, 0, 3, 0, 0)^T$ (stars) to $\boldsymbol{q}_f = (0, 0, 4, 0, 3, 4)^T$ (diamonds) with $\boldsymbol{v}_1(t_0) = (0, 0, 1)^T$, $\boldsymbol{v}_2(t_0) = (0, 0, -1)^T$, $\boldsymbol{v}_1(t_f) = (-1, 0, 0)^T$ and $\boldsymbol{v}_2(t_f) = (1, 0, 0)^T$. Furthermore, a maximum control magnitude of 1 as been considered.

through $\omega_{r,1} = -\omega_{r,2} = -\varepsilon$ that decreases the value of σ ensuring (3). Otherwise, if, and when, $\omega_i = \omega_M - \varepsilon$ the controls $\omega_{r,1} = \omega_{r,2} = 0$ are considered and the system evolves with constant σ (and θ) while $\boldsymbol{D}$ continues to perform a rotation thanks to $\boldsymbol{\omega}_{tr}$. As described in III-C, at the appropriate time $\bar{t} - \delta$ the controls $\omega_{r,1} = -\omega_{r,2} = -\varepsilon$ are then applied. Since the value of σ decreases (3) is ensured.

Step 4 of the Motion Planning algorithm is equivalent to a planar steering of a two 2D Dubins vehicles without rotations of $\boldsymbol{D}$, i.e. $\omega_{tr} = 0$. In the proposed algorithm, we choose to steer the system with circular arcs and straight lines choosing $\boldsymbol{\omega}_{r,1} = \boldsymbol{\omega}_{r,2}$ with magnitude smaller than ω_M, i.e. circular arcs of radius larger than R.

Concluding, critical configurations from a control point of view are either initial or final configurations.
If ω_{tr} is strictly smaller than ω_M, it is always possible to give the vehicles relative controls $\boldsymbol{\omega}_{r,i}$ in order to execute the proposed motion planning algorithm.

■

VI. Conclusions

In this paper a model for a *3D–Dubins* systems consisting of a pair of Dubins vehicles moving in a 3D space maintaining constant distance has been introduced with constraints on the control. A motion planning algorithm of the proposed system has been introduced based on three basic movements with associated control laws. A theorem providing sufficient conditions on the initial and final configurations that guarantees the existence of admissible controls has been demonstrated based on the proposed motion planning algorithm.

A necessary condition to ensure existence of admissible control is under investigation to have a complete controllability characterization. The results of this paper can be seen as a starting point to solve the motion planning and controllability problems for formations of multi-vehicle systems as it has been done in [12], [17] for the planar case.

Future developments will regard control laws that take into account more complex constraints depending on both states and controls, such as non uniform bounds on the control components and bounds on the roll angle.

Finally, the existence of a control that steers the system among feasible configurations is fundamental to solve the challenging optimal control problem, i.e. to determine the control law that steers the system as desired while minimizing a certain cost functional (e.g. time spent, distance travelled).

VII. Acknowledgments

The authors gratefully acknowledge H. Wang for the inspiring discussions at the base of this work.

References

[1] Y. Chen and Z. Wang, "Formation control: a review and a new consideration," in *Intelligent Robots and Systems, 2005.(IROS 2005). 2005 IEEE/RSJ International Conference on*. IEEE, 2005, pp. 3181–3186.

[2] F. Belkhouche, S. Vadhva, and M. Vaziri, "Modeling and controlling 3d formations and flocking behavior of unmanned air vehicles," in *Information Reuse and Integration (IRI), 2011 IEEE International Conference on*, aug. 2011, pp. 449 –454.

[3] M. Mesbahi and M. Egerstedt, *Graph theoretic methods in multiagent networks*. Princeton University Press, 2010.

[4] L. Consolini, F. Morbidi, D. Prattichizzo, and M. Tosques, "A geometric characterization of leader-follower formation control," in *Robotics and Automation, 2007 IEEE International Conference on*. IEEE, 2007, pp. 2397–2402.

[5] D. Scharf, F. Hadaegh, and S. Ploen, "A survey of spacecraft formation flying guidance and control. part ii: control," in *American Control Conference, 2004. Proceedings of the 2004*, vol. 4. IEEE, 2004, pp. 2976–2985.

[6] M. Abrahams and P. Colgan, "Fish schools and their hydrodynamic function: a reanalysis," *Environmental Biology of Fishes*, vol. 20, pp. 79–80, 1987.

[7] T. Balch and R. Arkin, "Behavior-based formation control for multi-robot teams," *IEEE Transactions on Robotics and Automation*, vol. 14, no. 6, pp. 926–939, 1998.

[8] A. Das, R. Fierro, V. Kumar, J. Ostrowski, J. Spletzer, and C. Taylor, "A vision-based formation control framework," *IEEE Transactions on Robotics and Automation*, vol. 18, no. 5, pp. 813–825, 2002.

[9] J. Desai, J. Ostrowski, and V. Kumar, "Modeling and control of formations of nonholonomic mobile robots," *IEEE transactions on Robotics and Automation*, vol. 17, no. 6, pp. 905–908, 2001.

[10] M. Lewis and K. Tan, "High precision formation control of mobile robots using virtual structures," *Autonomous Robots*, vol. 4, no. 4, pp. 387–403, 1997.

[11] T. Barfoot and C. Clark, "Motion planning for formations of mobile robots," *Robotics and Autonomous Systems*, vol. 46, no. 2, pp. 65–78, 2004.

[12] H. Wang, L. Pallottino, and A. Bicchi, "Controllability properties for aircraft formations," in *Decision and Control (CDC), 2010 49th IEEE Conference on*, dec. 2010, pp. 2047 –2054.

[13] R. Skjetne, S. Moi, and T. Fossen, "Nonlinear formation control of marine craft," in *Decision and Control, 2002, Proceedings of the 41st IEEE Conference on*, vol. 2, 2002.

[14] J. P. Laumond and S. Sekhavat, "Guidelines in nonholonomic motion planning for mobile robots," *Robot Motion Planning and Control*, pp. 1–53, 1998.

[15] H. Sussmann and G. Tang, "Shortest paths for the Reeds-Shepp car: a worked out example of the use of geometric techniques in nonlinear optimal control," Dept. of Mathematics, Rutgers University, Piscataway, NJ, Technical Report SYNCON 91-10, 1991.

[16] H. Wang, L. Pallottino, and A. Bicchi, "Controllability for pairs of vehicles maintaining constant distance," *IEEE International Conference on Robotics & Automation, 2010*, pp. 342–349, May 2010.

[17] ——, "Motion planning for formations of dubins vehicles," in *Decision and Control (CDC), 2010 49th IEEE Conference on*, dec. 2010, pp. 2263 –2269.

[18] S. Hota and D. Ghose, "Optimal geometrical path in 3d with curvature constraint," in *Intelligent Robots and Systems (IROS), 2010 IEEE/RSJ International Conference on*. IEEE, 2010, pp. 113–118.